

Dynamic functional connectivity changes associated with dementia in Parkinson's disease

Eleonora Fiorenzato,¹ Antonio P. Strafella,^{2,3,4} Jinhee Kim,^{2,3,4} Roberta Schifano,¹ Luca Weis,¹ Angelo Antonini⁵ and Roberta Biundo¹

Dynamic functional connectivity captures temporal variations of functional connectivity during MRI acquisition and it may be a suitable method to detect cognitive changes in Parkinson's disease. In this study, we evaluated 118 patients with Parkinson's disease matched for age, sex and education with 35 healthy control subjects. Patients with Parkinson's disease were classified with normal cognition ($n = 52$), mild cognitive impairment ($n = 46$), and dementia ($n = 20$) based on an extensive neuropsychological evaluation. Resting state functional MRI and a sliding-window approach were used to study the dynamic functional connectivity. Dynamic analysis suggested two distinct connectivity 'States' across the entire group: a more frequent, segregated brain state characterized by the predominance of within-network connections, State I, and a less frequent, integrated state with strongly connected functional internetwork components, State II. In Parkinson's disease, State I occurred 13.89% more often than in healthy control subjects, paralleled by a proportional reduction of State II. Parkinson's disease subgroups analyses showed the segregated state occurred more frequently in Parkinson's disease dementia than in mild cognitive impairment and normal cognition groups. Further, patients with Parkinson's disease dementia dwelled significantly longer in the segregated State I, and showed a significant lower number of transitions to the strongly interconnected State II compared to the other subgroups. Our study indicates that dementia in Parkinson's disease is characterized by altered temporal properties in dynamic connectivity. In addition, our results show that increased dwell time in the segregated state and reduced number of transitions between states are associated with presence of dementia in Parkinson's disease. Further studies on dynamic functional connectivity changes could help to better understand the progressive dysfunction of networks between Parkinson's disease cognitive states.

- 1 IRCCS San Camillo Hospital, Venice, Italy
- 2 Division of Brain, Imaging and Behaviour-Systems Neuroscience, Krembil Research Institute, UHN, University of Toronto, Toronto, ON, Canada
- 3 Research Imaging Centre, Campbell Family Mental Health Research Institute, Centre for Addiction and Mental Health, University of Toronto, Toronto, ON, Canada
- 4 Morton and Gloria Shulman Movement Disorder Unit and E.J. Safra Parkinson Disease Program, Neurology Division, Department of Medicine, Toronto Western Hospital, UHN, University of Toronto, Toronto, ON, Canada
- 5 Department of Neurosciences, University of Padua, Padua, Italy

Correspondence to: Roberta Biundo, PhD
IRCCS San Camillo Hospital, Via Alberoni 70, 30126 Venice, Italy
E-mail: roberta.biundo@yahoo.it

Keywords: Parkinson's disease; dynamic functional connectivity; mild cognitive impairment; dementia; neural networks

Abbreviations: AUD = auditory network; CB = cerebellar network; CEN = cognitive executive network; DFC = dynamic functional connectivity; DMN = default mode network; ICs = independent components; MCI = mild cognitive impairment; PD-MCI = Parkinson's disease with MCI; PDD = Parkinson's disease dementia; PD-NC = Parkinson's disease with normal cognition; SMN = sensorimotor network; VIS = visual network;

Introduction

Cognitive deficits in Parkinson's disease are characterized by marked heterogeneity, variable progression and discrete underlying pathology (Kehagia *et al.*, 2010; Aarsland *et al.*, 2017). Resting state functional MRI studies have indicated that alterations involve brain connectivity at rest and during the execution of specific tasks (Baggio *et al.*, 2014, 2015; Amboni *et al.*, 2015; Gorges *et al.*, 2015). However, functional MRI studies cannot provide the information necessary to understand the spatial-temporal aspects of information processing in the human brain. Functional MRI detects highly localized measures of brain activation, but its temporal resolution is much longer than the time needed for most perceptual and cognitive processes. Magnetoencephalography and EEG would have the necessary temporal resolution to study the dynamics of brain function, but their poor spatial resolution does not allow identification of underlying neural sources, particularly in the case of Parkinson's disease where degeneration involves both cortical and subcortical structures (Olde Dubbelink *et al.*, 2013; Babiloni *et al.*, 2017).

Temporal dynamic changes in brain network connectivity can be detected by analysing functional MRI acquisitions (Hutchison *et al.*, 2013; Allen *et al.*, 2014). Dynamic functional connectivity (DFC) alterations have been associated with specific cognitive states (Elton and Gao, 2015), psychiatric conditions (Damaraju *et al.*, 2014) and neurological disorders, such as Alzheimer's disease and Parkinson's disease (Jones *et al.*, 2012; Kim *et al.*, 2017; Cordes *et al.*, 2018; Diez-Cirarda *et al.*, 2018). Specifically, for Parkinson's disease, DFC studies suggested alterations from early Parkinson's disease stages (Cordes *et al.*, 2018), linked to disease progression (Kim *et al.*, 2017) and presence of mild cognitive deficits (Diez-Cirarda *et al.*, 2018). However, these studies were based on relatively small samples and included only non-demented Parkinson's disease.

The primary aim of this work was to investigate the differences in dynamic connectivity between healthy control subjects and patients with Parkinson's disease with adequate representation across the entire cognitive spectrum, ranging from normal cognition to dementia, using resting state DFC. We hypothesized that cognitive states in Parkinson's disease are linked to altered DFC temporal properties, which could possibly define functional neuroimaging biomarkers of cognitive decline and dementia.

Materials and methods

Participants

This study included 131 consecutive Parkinson's disease patients recruited from the Parkinson Disease and Movement Disorders Unit, Neurology Clinic Padua and San Camillo Hospital Venice between January 2013 and March 2017, and 36 healthy control subjects. Parkinson's disease was

diagnosed according to the UK Parkinson's Disease Society Brain Bank diagnostic criteria (Daniel and Lees, 1993). We excluded subjects with head injury history, presence of other significant psychiatric, neurological, or systemic comorbidity, MRI signal abnormalities (such as cerebral vascular lesions, white matter hyperintensities, and evidence of space-occupying lesions) and MRI artefacts. Further, we did not consider Parkinson's disease patients with deep brain stimulation and healthy control subjects with mild cognitive impairment (MCI) (Pedersen *et al.*, 2013). Healthy controls were matched to Parkinson's disease patients in terms of age, gender and education.

Disease severity was assessed using the motor section of the Movement Disorder Society Unified Parkinson's Disease Rating Scale (MDS-UPDRS-III) (Antonini *et al.*, 2012) and levodopa equivalent daily dosages were calculated for each patient (Tomlinson *et al.*, 2010).

The present study was approved by the Venice Research Ethics Committee, Venice, Italy. Written informed consent was obtained from all study subjects after full explanation of the procedure involved. The research was completed in accordance with the Declaration of Helsinki.

Neuropsychological and neuropsychiatric assessment

All subjects underwent a comprehensive neuropsychological battery as described previously (Biundo *et al.*, 2014), specifically designed to target cognitive deficits in Parkinson's disease according to level II criteria (Dubois *et al.*, 2007; Litvan *et al.*, 2012) (Supplementary material). Subjective cognitive complaints and their impact on functional autonomy were assessed during the clinical interview with the Parkinson's Disease Cognitive Functional Rating Scale (Kulisevsky *et al.*, 2013), as well as daily functioning (Katz, 1983).

First, *z*-scores were calculated for each test and subject, based on standardized published Italian norms that are adjusted for age and education. We classified Parkinson's disease patients as having MCI (PD-MCI) if *z*-score for a given test was at least 1.5 standard deviations (SD) below appropriate norms on two tests (i.e. within a single cognitive domain or at least one test in two or more cognitive domains) (Litvan *et al.*, 2012). Presence of Parkinson's disease dementia (PDD) was assessed based on the Movement Disorders Society Task force recommendations (Dubois *et al.*, 2007), which included cognitive, daily functioning and neuropsychiatric assessment. Patients without cognitive alterations were defined as Parkinson's disease with normal cognition (PD-NC). Further, *z* composite scores were computed to obtain global measures for each cognitive domain (i.e. attention/working memory, executive, memory, language and visuospatial/visuo-perceptive functions).

Data acquisition and preprocessing

Images were acquired on 1.5T Philips Achieva scanner (Philips Medical Systems) using an 8-channel head coil. Structural 3D T₁-weighted images were acquired with turbo field echo sequence with the following parameters: repetition time = 8.3 ms, echo time = 4.1 ms, flip angle = 8°, field of view = 250 × 250 mm, matrix resolution = 288 × 288, number

of slices = 187, voxel size = $0.87 \times 0.87 \times 0.87$ mm with no gap, number of total volumes = 240. Resting state data were acquired using an echo-planar imaging sequence with repetition time = 1939.4 ms, echo time = 45 ms, number of slices = 25, flip angle = 90° , field of view = 230×230 mm, matrix size = 80×80 , voxel size = $2.875 \times 2.875 \times 5.20$ mm with no gap, and sensitivity encoding factor = 2. Resting state scans were carried out in two consecutive scanning runs of ~ 8 min each. During functional MRI, participants were instructed to lie quietly with their eyes closed and without thinking about anything specific and to avoid falling asleep, confirmed by post-scan debriefing. Headphones were used to attenuate scanner noise and head motion was restrained with foam padding; further, patients with Parkinson's disease were ON dopaminergic medication during MRI scanning to control for involuntary head motions.

Data preprocessing was carried out using SPM12 software (<http://www.fil.ion.ucl.ac.uk/spm/>) implemented in MATLAB (version R2016b, MathWorks, Inc., Natick, MA, USA). Data were realigned to the first volume to correct for interscan head motions, segmented into grey matter, white matter and CSF using the Tissue Probability Map template, normalized into standard Montreal Neurological Institute space using non-linear transformations and smoothed with a Gaussian smoothing kernel of 6 mm full-width at half-maximum.

Image quality and motion control

Before data preprocessing, we carried out image quality control and discarded images with signal dropout in one of the two scanning runs. As excessive head motion can significantly affect DFC analyses (Van Dijk *et al.*, 2012; Hutchison *et al.*, 2013), we applied conservative inclusion criteria to minimize potential head-motion bias. Namely, we calculated mean framewise displacement and maximum displacement. The former index was calculated using the published formula of Power *et al.* (2012), as a combination of translational (x , y , z axes) and rotational (pitch, yaw, roll) scan-to-scan displacement, using the six parameters obtained for each subject during the realignment steps. Maximum displacement was defined as the maximum absolute translation of each volume compared to the reference volume in x , y and z directions.

Acquisitions were discarded if they had mean framewise displacement values > 0.2 mm, or if maximum displacement was greater than one voxel size, or if outliers accounted for $> 30\%$ of the whole sample, in at least one of the two scanning runs. According to these criteria, we excluded 14 acquisitions from 13 patients with Parkinson's disease and one healthy control.

Group independent component analysis

After data preprocessing, resting state data of all participants were analysed using spatial independent component analysis as implemented in the GIFT software (Calhoun *et al.*, 2001a; Erhardt *et al.*, 2011) to decompose the data into functional networks that exhibited a unique time course profile.

Two data reductions steps were carried out in the principal component analysis, subject-specific and group-level steps. First, subject-specific data were reduced to 120 components and subject-reduced data were concatenated across time.

Further, at group level, data were reduced into 100 group independent components (ICs) with the expectation-maximization algorithm, included in GIFT (Roweis, 1998). Reliability and stability of the *infomax* independent component analysis algorithm in ICASSO (Bell and Sejnowski, 1995) was ensured by repeating the independent component analysis algorithm 20 times (Himberg *et al.*, 2004).

The resulting components were clustered to estimate their reliability and components with values > 0.80 were selected. Subject-specific spatial maps and time courses were obtained using the back-reconstruction approach (GICA) (Calhoun *et al.*, 2001b).

Among the 100 independent components, we identified relevant intrinsic connectivity networks by applying a previously described procedure (Allen *et al.*, 2014). We first manually confirmed if the peak activation coordinates were located primarily in grey matter, showing low spatial overlap with vascular, ventricular, edge regions corresponding to artefacts (Allen *et al.*, 2011) and then if time course was dominated by low-frequency fluctuations, with ratio of power < 0.10 Hz to 0.15–0.25 Hz (Cordes *et al.*, 2000). This process resulted in 35 meaningful independent components that we sorted into seven functional networks, based on the spatial correlation values between independent components and the template (Shirer *et al.*, 2012; Allen *et al.*, 2014). As shown in Fig. 1 and Supplementary Table 1, the functional networks were arranged into: basal ganglia, auditory (AUD), visual (VIS), sensorimotor (SMN), cognitive executive (CEN), default mode (DMN), and cerebellar (CB) networks.

As shown by Allen *et al.* (2014), additional postprocessing was applied to the time courses of 35 independent components to remove remaining noise sources. Independent component time courses were detrended, despiked using AFNI's 3dDespike algorithm, filtered using a fifth order Butterworth filter with a 0.15 Hz high frequencies cut-off, and finally we regressed out the movement parameters.

Dynamic functional connectivity

Sliding window approach

The most common way to investigate DFC is the sliding window approach; we computed this analysis using the DFC network toolbox in GIFT. In line with previous studies (Allen *et al.*, 2014; Damaraju *et al.*, 2014; Kim *et al.*, 2017), resting state data were divided into windows of 22 repetition times (44 s) size, in steps of one repetition time, as this segment length has been demonstrated to provide a good compromise between the quality of correlation matrix estimation and the ability to resolve dynamics (Allen *et al.*, 2014). In this regard, cognitive states seem to be identified at window lengths of 30–60 s, while topological assessments of brain networks begin to be stabilized at ~ 30 s (Jones *et al.*, 2012; Shirer *et al.*, 2012). As covariance estimation using shorter time series can be noisy, the regularized inverse covariance matrix was used (Varoquaux *et al.*, 2010; Smith *et al.*, 2011). Further, we imposed an additional L1 norm of the precision matrix to promote sparsity in the graphic LASSO framework with 100 repetitions (Friedman *et al.*, 2008). After computing DFC, all the functional connectivity matrices were transformed to z -scores using Fisher's z -transformation to stabilize variance prior to further analysis. Fisher z -transformed matrices were

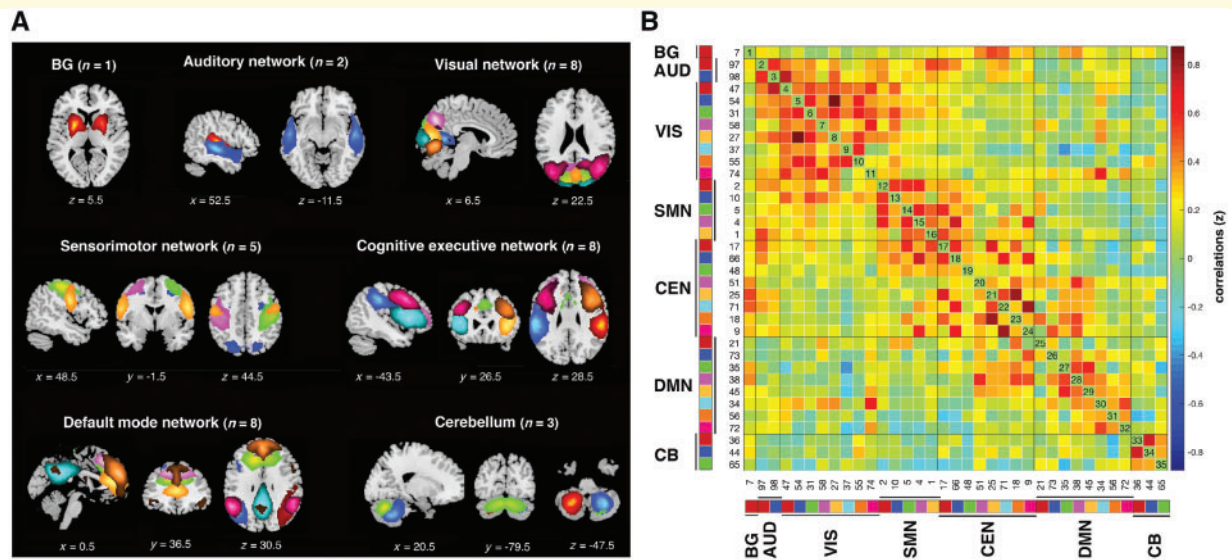


Figure 1 Independent components ($n = 35$) identified by group independent component analysis. **(A)** Independent component spatial maps divided on seven functional networks [basal ganglia (BG), AUD, VIS, SMN, CEN, DMN and CB] based on their anatomical and functional properties. **(B)** Group averaged static functional connectivity between independent component pairs was computed using the entire resting state data. The value in the correlation matrix represents the Fisher's z-transformed Pearson correlation coefficient. Each of the 35 independent components was rearranged by network group based on the seven functional networks.

then residualized with nuisance variables, such as age and gender (Allen *et al.*, 2011).

Clustering analysis

Following a previous study (Allen *et al.*, 2014), we applied a k -means clustering algorithm on windowed functional connectivity matrices (Lloyd, 1982), to assess the reoccurring functional connectivity patterns (states), as expressed by the frequency and structure of these states. We used L1 distance (Manhattan distance) function to estimate the similarity between window functional connectivity matrices, as it has been demonstrated to be an effective measure for high-dimensional data (Aggarwal *et al.*, 2001). Further, to estimate the optimal number of clusters, a cluster validity analysis (silhouette) was carried out on the exemplars of all the subjects. We used the subset of windows (consisting of local maxima in functional connectivity variance) as subject exemplars to decrease the redundancy between windows and computational demands (Allen *et al.*, 2014). As shown by others, subsampling produced reliable results from whole windows and without biasing group clusters (Allen *et al.*, 2014), and thus the reproducibility of functional connectivity states was established using replication on bootstrap resampling and split-half sample methods.

As in a previous study (Kim *et al.*, 2017), we determined the optimal number of clusters as equal to two ($k = 2$), based on the silhouette criterion of cluster validity index (Rousseeuw, 1987), computed as how similar a point is to other points in its own cluster, when compared to points in other clusters.

Group differences in dynamic connectivity: temporal properties and strength

We investigated the temporal properties of DFC states by computing the average dwell time and fractional windows in each state, as well as the number of transitions from one state to another. Mean 'dwell time' is defined as the number of consecutive windows belonging to one state, 'fractional windows' as the number of total windows belonging to one state, and 'number of transitions' is defined as the number of transitioning between states and represents the reliability of each state. We tested if there were any differences between the two scanning runs on these temporal measurements, by performing a repeated-measures ANOVA, using the two scanning runs as within-subject factor. Group differences in dwell time, fractional windows and number of transitions, between age-, gender-, and education-matched healthy controls and Parkinson's disease patients were examined using a two-sample t -test [$P < 0.05$, false discovery rate (FDR) correction]. Between-group differences among the Parkinson's disease subgroups (PD-NC, PD-MCI and PDD) were investigated using an analysis of covariance and including education, levodopa and dopamine agonist equivalent daily doses as covariates ($P < 0.05$, FDR correction).

Subject-specific medians corresponding to each group-level state were estimated and two sample independent t -tests were used to compare the connectivity strength of each state at each unique regional pairing (595 pairings; $P < 0.05$, FDR correction) between groups.

Further, ANOVA was run to compare strength abnormalities associated with cognitive deficits by comparing Parkinson's disease subgroups ($P < 0.05$, FDR correction).

Clinical and neuropsychological data analysis

Statistical analyses were performed using SPSS Statistic, release version 24.0 (Chicago, IL, USA). Healthy control subjects and patients with Parkinson's disease were compared using Student's *t*-test, while Parkinson's disease subgroups were compared across cognitive states (PD-NC, PD-MCI and PDD) with three-level one-way ANOVAs. To compare all four subgroups (healthy controls, PD-NC, PD-MCI and PDD), four-level one-way ANOVAs were run. Pearson's chi-square test was used to compare categorical variables. We carried out Pearson's correlation analyses between altered temporal properties and cognition in the whole group [Montreal Cognitive Assessment (MoCA), Mini-Mental State Examination (MMSE) and cognitive performance in each domain] as well as motor severity (MDS-UPDRS-III) in Parkinson's disease. Statistical significance threshold was set at $P < 0.05$ and corrected for multiple comparisons.

Data availability

Data supporting the findings of this study are available from the corresponding author, upon reasonable request.

Results

Demographic, clinical and cognitive characteristics

Our sample consisted of 35 healthy controls and 118 patients with Parkinson's disease. No significant differences were found between healthy controls and Parkinson's disease patients as whole group (Supplementary Table 2), in age, education and gender. Forty-six patients (39.0%) fulfilled the criteria for MCI, 20 (16.9%) for dementia and the remaining 52 (44.1%) were cognitively normal (Table 1).

Neuropsychological differences between groups

Table 2, Fig. 2 and Supplementary Tables 3 and 4 show differences in neuropsychological performance between groups. Patients with PDD were mainly impaired in attention/working-memory domain (84.2%), followed by memory (72.2%), executive, visuospatial (70.6%), and language abilities (38.9%). In the PD-MCI group, attention/working memory was the most impaired domain (42.2%), followed by the visuospatial (40.0%), memory, executive and language abilities (26.1%, 22.2%, 8.7%, respectively). There was no difference between healthy controls and PD-NC.

Intrinsic connectivity networks

Spatial maps of all 35 independent components, identified using the group independent component analysis, are shown in Fig. 3. Independent components were grouped in the following seven networks based on their anatomical and presumed functional properties: basal ganglia (IC 7), AUD (ICs 97, 98), VIS (ICs 47, 54, 31, 58, 27, 37, 55, 74), SMN (ICs 2, 10, 5, 4, 1), CEN (ICs 17, 66, 48, 51, 25, 71, 18, 9), DMN (21, 73, 35, 38, 45, 34, 56, 72), and CB (36, 44, 65). The detailed information and spatial maps of independent components are listed in Supplementary Table 1 and Supplementary Fig. 1.

Dynamic functional connectivity state analysis

Temporal properties

We identified two patterns of structured functional connectivity states, recurring during individual scans, across subjects and between the two scanning runs. Namely, a more frequent and relatively sparsely connected State I, and a less frequent and stronger interconnected State II. The percentages of total occurrences of these two states were quite different, with State I more frequent (66%) than State II (34%). Figure 3 shows these two common functional connectivity states and the corresponding visualized connectivity patterns (centroids of clusters). Within-group repeated measure ANOVA excluded that differences in the temporal properties were related to the scanning runs and a relation with groups.

Figure 4A and B shows state- and group-specific cluster centroids obtained by the k-means cluster analysis. We observed that in healthy controls and Parkinson's disease patients, State I was characterized by sparse interindependent component connections that were located mostly within each network (AUD, VIS, SMN, CEN, DMN and CB), while stronger internetwork connections were observed in State II, involving the AUD, VIS, SMN, CEN and DMN networks. In Parkinson's disease, State I was more frequently observed ($69.42 \pm 27.10\%$) than State II ($30.58 \pm 27.10\%$); whereas in healthy controls, State I occurred less frequently ($55.53 \pm 26.43\%$) ($P = 0.008$) and State II more commonly ($44.47 \pm 26.43\%$) ($P = 0.008$) compared to Parkinson's disease (Fig. 5A).

Further, State I was more frequent in PDD ($83.65 \pm 21.70\%$) than in PD-MCI ($65.19 \pm 29.12\%$) and PD-NC ($67.69 \pm 25.65\%$) ($P < 0.05$, FDR correction); while the opposite pattern was observed for State II, which was less frequent in PDD ($16.35 \pm 21.70\%$) than in PD-MCI ($34.81 \pm 29.21\%$) and PD-NC ($32.31 \pm 25.65\%$) ($P < 0.05$, FDR correction).

As reported in Fig. 5B, significant group differences (Parkinson's disease versus healthy controls) were identified in the mean dwell time of State I. Specifically, the Parkinson's disease group showed a significantly longer mean dwell time

Table 1 Demographic and clinical data from study groups

	Healthy controls (n = 35)			PD-NC (n = 52)			PD-MCI (n = 46)			PDD (n = 20)			HC versus PD-MCI P-value	HC versus PD-NC PDD	PD-NC versus PD-MCI PDD	PD-NC versus PDD
	Mean (SD)	Min-max		Mean (SD)	Min-max		Mean (SD)	Min-max		Mean (SD)	Min-max					
Age	61.29 (8.98)	45–83		58.63 (9.58)	34–85		65.87 (11.37)	36–81		71.75 (6.62)	55–82		–	0.0011	0.0020	<0.0001
Education	12.43 (4.02)	5–18		12.67 (3.86)	5–18		9.61 (4.49)	2–18		8.45 (4.36)	3–18		0.0178	0.0050	0.0023	0.0010
Sex (m/f)	18/17	–		–	–		33/13	–		13/7	–		–	–	–	–
Disease duration	–	–		9.48 (4.62)	1–20		9.09 (5.4)	2–28		12.35 (6.35)	4–23		–	–	–	–
Age of onset	–	–		49.19 (9.45)	29–73		56.57 (13.54)	13–75		59.4 (10.58)	40–78		–	–	0.0054	0.0027
MDS-UPDRS-III	–	–		16.41 (8.53)	4–41		26.82 (15.04)	7–68		35.6 (16.71)	12–77		–	–	0.0011	<0.0001
LEDD	–	–		859.23 (553.97)	0–2080		947.92 (485.81)	60–2296		824.15 (472.84)	150–1955		–	–	–	–
DAED	–	–		160.19 (113.19)	0–480		143.24 (112.23)	0–390		60 (88.74)	0–240		–	–	–	0.0030
ADL	6 (0)	6–6		5.73 (0.79)	1–6		5.7 (0.47)	5–6		4.1 (1.77)	1–6		–	<0.0001	–	<0.0001
IADL	6.54 (1.52)	5–8		5.81 (1.48)	1–8		5.39 (1.61)	2–8		3.15 (1.73)	0–6		0.0077	<0.0001	–	<0.0001
PD-CFRS	–	–		2.09 (2.26)	0–9		3.25 (2.49)	0–10		12.42 (5.78)	2–21		–	–	–	<0.0001
PDQ-8	–	–		9.04 (5.19)	0–22		8.28 (5.13)	0–18		12.88 (6.14)	3–23		–	–	–	0.0412
Apathy scale	10.58 (4.23)	4–21		12.83 (5.84)	3–29		12.47 (5.47)	3–26		17.23 (6.15)	7–33		–	0.0036	–	–
STAI-Y1	33.64 (9.28)	20–54		37.63 (10.85)	20–69		36.88 (10.02)	20–62		41.4 (8.65)	29–56		–	–	–	–
STAI-Y2	39.42 (10.13)	22–67		40.73 (10.66)	20–63		40.88 (11.4)	20–62		41.29 (8.33)	29–60		–	–	–	–
BDI-II	7.6 (7.47)	0–32		8.88 (7.44)	0–32		10.7 (7.57)	1–36		15.44 (7.4)	3–33		–	0.0025	–	0.0099
BIS-11	58.03 (9.83)	44–82		61 (9.68)	45–84		58.68 (8.57)	39–77		62.1 (7.85)	49–74		–	–	–	–
MIMSE	29.03 (1.38)	23–30		28.87 (1.07)	26–30		26.83 (2.32)	20–30		22.4 (3.07)	17–27		<0.0001	<0.0001	<0.0001	<0.0001
MoCA	25.86 (2.58)	19–30		25.62 (2.15)	21–30		21.11 (4.21)	11–29		15.15 (3.98)	9–22		<0.0001	<0.0001	<0.0001	<0.0001

One-way ANOVA was run to test between-group differences (HC, PD-NC, PD-MCI, and PDD). Chi-square test was used for categorical variables. Multiple comparisons correction was applied to control for the number of intergroup comparisons. No differences between healthy controls versus PD-NC were found.

ADL = activities of daily living; BDI-II = Beck Depression Inventory-II; BIS-11 = Barratt Impulsiveness Scale; DAED = dopamine agonist equivalent dose; HC = healthy controls; IADL = Instrumental activities of daily living; LEDD = levodopa equivalent daily dose; MDS-UPDRS = Movement Disorder Society Unified Parkinson's Disease Rating Scale; MIMSE = Mini-Mental State Examination; MoCA = Montreal Cognitive Assessment; PD-CFRS = Parkinson's Disease -Cognitive Functional Rating Scale; PDQ-8 = Parkinson's Disease Questionnaire; STAI (Y-1, Y-2) = State-Trait Anxiety Inventory.

in State I (Parkinson's disease: 75.48 ± 58.67 , healthy controls: 46.39 ± 39.60 ; $P = 0.007$), while there was a trend for a longer mean dwell time in State II in the healthy controls group (healthy controls: 30.13 ± 24.43 , Parkinson's disease: 23.10 ± 24.48 ; $P = 0.137$).

Between-group comparisons among Parkinson's disease subgroups revealed that patients with PDD spent significantly more time in State I than PD-MCI and PD-NC patients (PDD: 115.75 ± 63.80 , PD-MCI: 67.51 ± 53.12 , PD-NC: 67.05 ± 55.91 , $P < 0.05$, FDR correction), and less time in State II as compared to PD-MCI (PDD: 12.88 ± 17.26 , PD-MCI: 29.72 ± 31.08 , $P < 0.05$, FDR correction) and PD-NC, although the latter was seen only as a trend (PDD: 12.88 ± 17.26 , PD-NC: 21.18 ± 18.08 , $P = 0.080$).

Healthy controls (5.94 ± 2.32) changed more frequently between brain states than patients with Parkinson's disease (4.59 ± 2.64) ($P = 0.007$). Finally, the Parkinson's disease subgroup analysis unveiled that the PDD group made fewer transitions compared to the PD-MCI and PD-NC groups (PDD: 3.20 ± 2.28 , PD-MCI:

4.59 ± 2.65 , PD-NC: 5.13 ± 2.62 , $P < 0.05$, FDR correction) (Fig. 5C).

Overall, these changes in DFC suggested that Parkinson's disease patients with major cognitive alterations stay longer in State I, which is characterized by sparsely within-network functional connectivity, making fewer transitions and dwelling shorter in the strongly interconnected State II.

Strength of dynamics states

We compared the strength of connections in the Parkinson's disease and healthy control groups among states. For State I, we observed 60 stronger within- and between-network connections in healthy controls compared to patients with Parkinson's disease (healthy controls $>$ Parkinson's disease, $P < 0.0125$, FDR correction). Twenty per cent of these connections were within-network (SMN and DMN); the remaining were between-networks (AUD-VIS, AUD-SMN, VIS-SMN, VIS-DMN, VIS-CEN, SMN-CEN, CEN-DMN, CEN-CB and DMN-CB). We also observed 13 between-network connections, which were stronger in Parkinson's disease patients compared to healthy controls (SMN-CEN, VIS-DMN, SMN-DMN, AUD-DMN, CEN-DMN, SMN-CB, CEN-CB) (Parkinson's disease $>$ healthy controls, $P < 0.05$, FDR correction) (Fig. 4B).

In addition, the 56.67% (34/60) of healthy controls $>$ Parkinson's disease connections positively correlated ($P < 0.05$, FDR correction) with attentive, executive, memory and/or visuospatial domains—while 46.1% (6/13) of Parkinson's disease $>$ healthy controls connections correlated negatively ($P < 0.05$, FDR correction) with attentive, memory and/or visuospatial domains. Interestingly, 23% of these Parkinson's disease $>$ healthy controls connections were between DMN and CEN networks, which are normally displayed as anti-correlations.

Table 2 Percentages of patients with z-scores below -1.5 SD in each cognitive domain and across cognitive states

	PD-NC (n = 52)	PD-MCI (n = 46)	PDD (n = 20)
Attention/working memory	0%	42.0%	84.2%
Executive	3.8%	22.0%	70.6%
Visuospatial	1.9%	40.0%	70.6%
Memory	3.8%	26.1%	72.2%
Language	0%	8.7%	38.9%

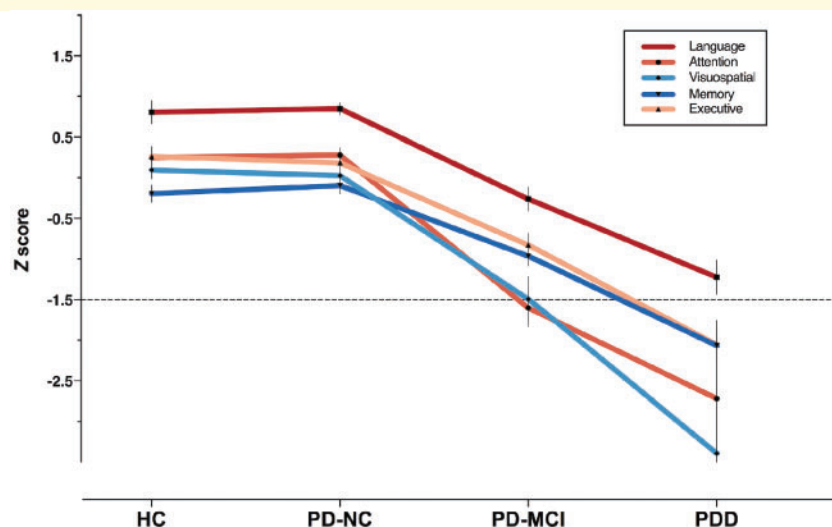


Figure 2 Neuropsychological performance in each cognitive domain as assessed by z composite score. HC = healthy controls.

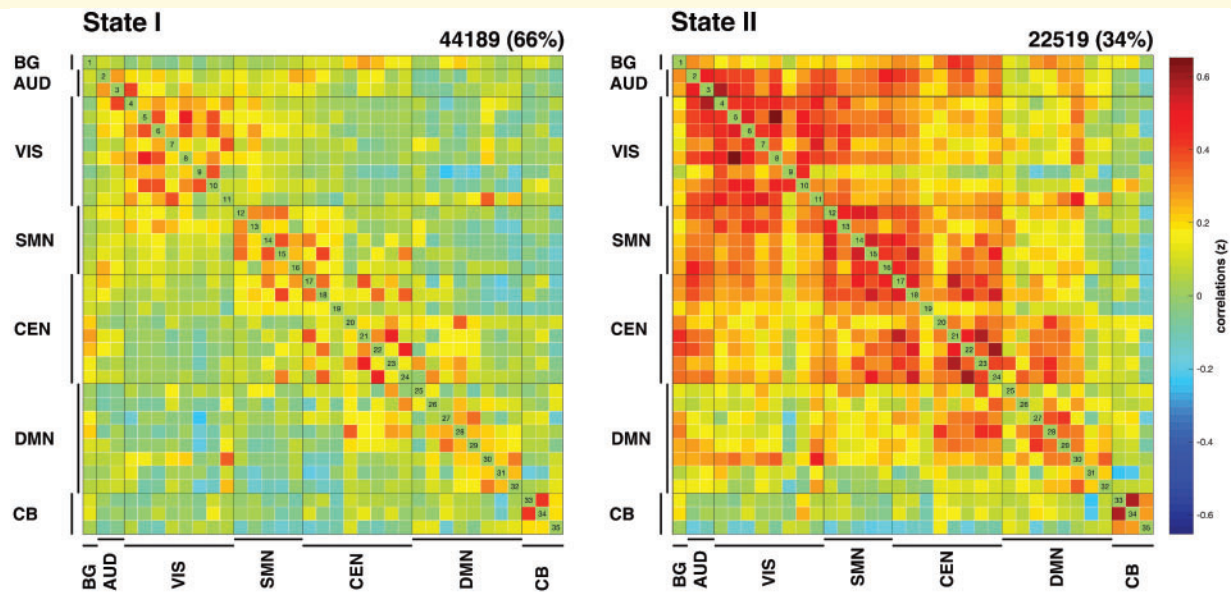


Figure 3 Results of the clustering analysis per state. Cluster centroids for each state. The total number of occurrences and percentage of total occurrences are listed above each cluster median. BG = basal ganglia.

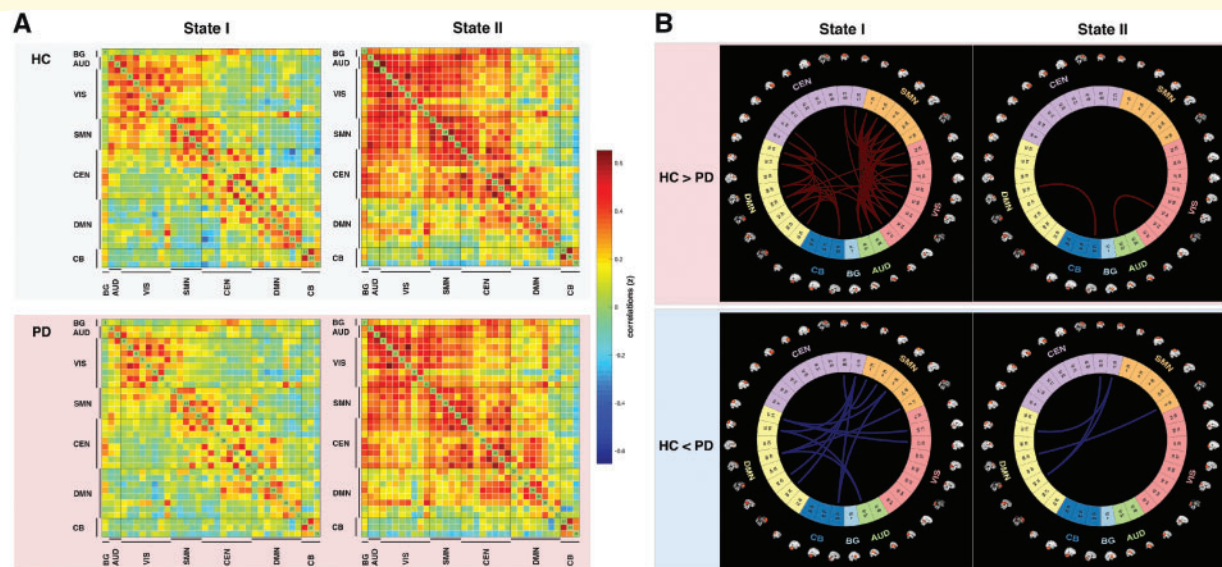


Figure 4 Functional connectivity state results. (A) Group centroid matrices for each state [percentage of total occurrences for states I and II: 55.5% and 44.5% in the healthy controls and 69.4% and 30.6% in the Parkinson's disease groups, respectively]. (B) Functional connectivity in each state, where Parkinson's disease had a weaker or stronger functional connectivity pattern in comparison to the healthy controls group. BG = basal ganglia; HC = healthy controls; PD = Parkinson's disease.

Overall these analyses suggest that poorer Parkinson's disease cognitive performance could be associated with alterations in the strength of connections. In particular, Parkinson's disease > healthy controls connections in DMN and CEN networks are possibly associated with the underlying cognitive deficits in Parkinson's disease.

Further, when we compared the strength of connection across Parkinson's disease cognitive states, there were no significant differences except for the within-network (VIS) connection (PDD < PD-MCI < PD-NC), which positively correlated with all cognitive domains.

Repeating the same analyses for State II, we found that healthy controls had two stronger between-network

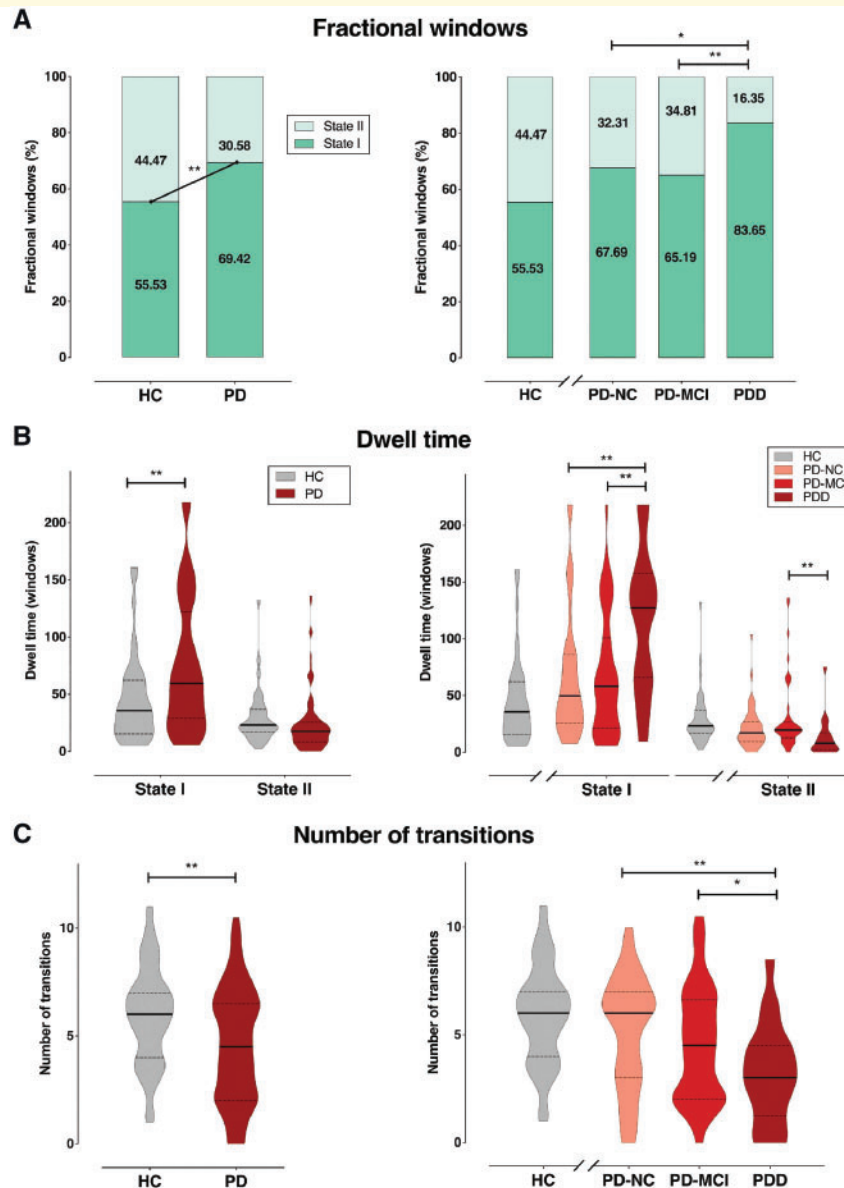


Figure 5 Temporal properties of DFC states for the Parkinson's disease and healthy control groups, and across Parkinson's disease cognitive states. **(A)** Percentage of total time subjects spent in each state. **(B)** Mean dwell time and **(C)** number of transitions between states were plotted using violin plots. Horizontal lines indicate group medians and interquartile range (solid and dashed line, respectively). * $P < 0.05$, ** $P < 0.01$. HC = healthy controls; PD = Parkinson's disease.

connections compared to Parkinson's disease patients (AUD-VIS and DMN-CB) ($P < 0.0125$, FDR correction), while Parkinson's disease had stronger connections in CEN-DMN and DMN-SMN networks, again suggesting increased activity in networks that are normally anti-correlated. However, these State II connections did not correlate with any cognitive domain. Finally, we did not find any differences in strength of connections across Parkinson's disease cognitive states except in the VIS-DMN internetwork (PDD $<$ PD-MCI $<$ PD-NC), which positively correlated with the cognitive performance in the attentive, memory and language domains ($P < 0.05$, FDR correction).

Correlation between clinical measures and dynamic functional connectivity properties

Correlation analyses were carried out to test whether DFC properties were associated with clinical characteristics. Notably, we found that dwell time in State I was negatively correlated with cognitive performance on the attention/working memory, executive, memory and visuospatial domains, as well as on global cognitive scales (MMSE and MoCA) (Table 3). This means that worse cognitive performance associated with long time spent in the more

Table 3 Correlations between dynamic functional connectivity temporal properties and clinical characteristics

		MDS-UPDRS III ^a	MoCA	MMSE	Cognitive domains				
					Attention/ working memory	Executive	Memory	Language	Visuospatial memory
Dwell time State I	r	0.143	−0.256	−0.202	−0.170	−0.169	−0.248	−0.158	−0.270
	P-value	0.159	0.001	0.012	0.035	0.037	0.002	0.051	0.001
Dwell time State 2	r	−0.070	0.178	0.090	0.000	0.060	0.097	0.049	0.109
	P-value	0.496	0.027	0.269	0.998	0.458	0.232	0.544	0.181
Fractional windows	r	0.141	−0.242	−0.159	−0.138	−0.165	−0.186	−0.130	−0.200
	P-value	0.167	0.003	0.050	0.089	0.041	0.021	0.108	0.014
Number of transitions	r	−0.152	0.229	0.218	0.242	0.229	0.252	0.189	0.243
	P-value	0.135	0.004	0.007	0.003	0.004	0.002	0.019	0.003

Pearson's correlation test was used, followed by multiple comparisons correction.

^aCorrelation performed for the Parkinson's disease group ($n = 118$). Significant results are reported in bold type.

MDS-UPDRS = Movement Disorder Society Unified Parkinson's Disease Rating Scale; MMSE = Mini-Mental State Examination; MoCA = Montreal Cognitive Assessment.

sparsely within-network connected State I. On the contrary, dwell time in State II did not correlate with cognitive scores. We found negative associations between fractional windows and cognitive performance on memory, visuospatial domains as well as on MoCA, suggesting that a higher percentage of total time spent in each state was associated with poorer cognitive function. Further, the number of transitions was positively associated with cognitive performance (on all cognitive domains and global cognitive scales). Additionally, it is worth noting the temporal properties of DFC did not correlate with MDS-UPDRS-III.

Discussion

This is the first study in a large Parkinson's disease and healthy controls cohort that applied a DFC analysis to identify differences in the dynamic connectivity across Parkinson's disease cognitive states, ranging from normal cognition to dementia, with a focus on the temporal properties (fractional windows, dwelling time, number of transitions) and on the strength of functional connectivity states.

We found two distinct connectivity states across the entire group. A more frequent brain state characterized by the predominance of within-network connections, State I, or segregated state; and a less frequent brain state characterized by the prevalence of strong connections between distinct functional network components, State II, or integrated state. We observed that in patients with Parkinson's disease, State I occurred 13.89% more often than in healthy controls, and the expression of integrated State II was lower. Specifically, the occurrence of the segregated State I was observed more frequently in PDD, paralleled by a proportional decreased expression of the integrated state, suggesting that reduced 'crosstalk' between brain networks and increased segregation were associated with cognitive decline. This confirms our hypothesis of altered

temporal properties in dynamic connectivity in association with Parkinson's disease significant cognitive dysfunctions. Our results are consistent with the DFC study by Diez-Cirarda *et al.* (2018), who found functional connectivity alterations in Parkinson's disease with MCI. Both studies showed that significant altered dynamic temporal properties can be seen in Parkinson's disease patients with greater cognitive severity. However, they did not include patients with dementia and their cohort might have been too small to detect differences between PD-NC and PD-MCI in the *post hoc* analysis.

There is growing evidence of an altered resting state connectivity pattern associated with cognitive impairments in Parkinson's disease (Baggio *et al.*, 2014, 2015; Amboni *et al.*, 2015; Gorges *et al.*, 2015). Our findings are consistent with a previous functional networks study, using graph-theoretical analyses, wherein Parkinson's disease with cognitive deficits showed increased local connectivity (modularity and small-worldness) and altered long-range connectivity (Baggio *et al.*, 2014). In this regard, Göttlich *et al.* (2013) described Parkinson's disease as a 'disconnection syndrome', characterized by increased connectivity within the sensorimotor network and reduced interaction with other brain modules. Therefore, our findings add to the view that Parkinson's disease-associated dementia is characterized by a more segregated brain state compared to PD-MCI and PD-NC.

This is in line with evidence suggesting that integrative between-network communication is crucial for efficient cognition while within-network communication is crucial for motor execution (Cohen and D'Esposito, 2016). Interestingly, we found that increased brain network functional segregation was closely linked with cognitive performance, but not with motor dysfunctions (as assessed by MDS-UPDRS-III), corroborating the independence of motor-associated network (Niethammer and Eidelberg, 2012; Kim *et al.*, 2017; Schindlbeck and Eidelberg, 2018). However, we cannot fully exclude that the lack of

an association with the MDS-UPDRS-III is due to basal ganglia network parcellation.

Further, we observed that, patients with Parkinson's disease have overall significantly different DFC temporal properties than controls. Namely, the former dwelled longer in the segregated State I, and showed a lower number of transitions to the strongly interconnected state compared to healthy participants. These temporal dynamic differences were mainly driven by PDD patients, who spent more time in the State I and remained for a shorter period in the strongly interconnected State II, than PD-MCI and PD-NC.

These results are consistent with those obtained in other neurological (Alzheimer's disease and epilepsy) and psychiatric (schizophrenia) conditions, all showing altered mean dwelling time (Jones *et al.*, 2012; Damaraju *et al.*, 2014; Liu *et al.*, 2017; Lottman *et al.*, 2017; Diez-Cirarda *et al.*, 2018) and number of transitions compared to controls (Liu *et al.*, 2017; Diez-Cirarda *et al.*, 2018). In healthy controls, probability of transitioning positively correlated with executive function measures, indicating greater functional dynamics and cognitive flexibility (Nomi *et al.*, 2017). Moreover, in epileptic patients, higher number of transitions was inversely associated with disease duration (Liu *et al.*, 2017). Thus, aligned with these reports, our findings lead us to suggest that reduction in transitioning between brain states differentiates demented from non-demented Parkinson's disease patients, but is not able to differentiate patients with preserved cognition and PD-MCI. PDD patients are characterized by the lowest rate of transitions, possibly as a measure of reduced cognitive flexibility.

In addition, DFC temporal properties were closely associated with cognitive performance on several domains (i.e. attention, executive, memory and visuospatial). Indeed, worsening of cognitive performance correlated with higher State I proportion in the fractional windows, increased dwell time and reduction in the number of transitions in this segregated state. Taken together, these findings confirm the vulnerability of the resting state network in Parkinson's disease with cognitive deficits (Baggio *et al.*, 2014, 2015; Amboni *et al.*, 2015) and underline the importance of investigating Parkinson's disease-related cognitive signature to temporal dynamic of functional connectivity. Hence, prospective studies are needed to determine whether functional segregation as well as decreased number of transitions between states can be a potential biomarker of cognitive decline in Parkinson's disease.

Moreover, we observed that healthy controls segregated State I was generally characterized by stronger within- and between-network connections compared to Parkinson's disease patients who, conversely, showed only few stronger connections than healthy controls. These were associated with worse cognitive performance in the attentive, memory and visuospatial domains and a subset of these connections was located between DMN and CEN networks, which are usually characterized by anticorrelations (Fox *et al.*, 2009; Raichle, 2015). These findings emphasize that cognitive deficits in Parkinson's disease are also characterized by a reduction of

the normal decoupling between DMN and CEN (Baggio *et al.*, 2015). Finally, we found a weaker connection in the PDD group within the visual network in State I and between the VIS-DMN in State II compared to the other patients, which may express poor visual information processing.

There are a few limitations and shortcomings in the present work that have to be considered. First, patients were taking their normal dose of dopaminergic medication during the resting state MRI to reduce discomfort, motion artefacts as well as for ethical reasons (Van Dijk *et al.*, 2012). We cannot exclude that dopaminergic therapy had some effect on functional connectivity (Berman *et al.*, 2016) and possibly increased connectivity (Esposito *et al.*, 2013; Prodoehl *et al.*, 2014), reducing the magnitude of the observed effect. Second, it has been suggested that DFC analyses should be performed in resting state acquisitions of at least 10 min (Hindriks *et al.*, 2016). The length of our resting state acquisitions was 8 min, which according to recent evidence, allows stable static resting state functional MRI data (Tomasi *et al.*, 2016). In addition, we acquired two scanning runs for each participant (16 min per subject) and checked for the consistency of the analyses, as reported above. We acknowledge our data were acquired with 1.5 T MRI, as other recent DFC studies, which used magnetic resonance scanners with the same field strength (Demirtas *et al.*, 2016; Allen *et al.*, 2018). Further, our voxel dimension and repetition time did not differ from other 3 T MRI studies (Kim *et al.*, 2017), minimizing possible bias in independent components discrimination.

To summarize, this is the first large study to assess dynamic connectivity properties across the Parkinson's disease cognitive spectrum, ranging from normal cognition to dementia. Importantly, we have shown that temporal properties of functional dynamics (fractional windows, dwelling time and number of transitions) are altered in Parkinson's disease versus healthy controls as well as in patients with Parkinson's disease and dementia. Our findings show that increased dwell time in the segregated state and reduced number of transitions between states were associated with presence of dementia in Parkinson's disease. We believe this approach, particularly the temporal dynamics of functional connectivity, could be a useful imaging biomarker to monitor cognitive changes in Parkinson's disease.

Acknowledgements

We are grateful to all of the study participants for their patience and cooperation.

Funding

R.B. is supported by the Ministry of Health under Grant Number GR-2016-02361986. A.P.S. is supported by Canadian Institutes of Health Research (MOP-136778) and Canada Research Chair Program.

Competing interests

The authors report no competing interests.

Supplementary material

Supplementary material is available at *Brain* online.

References

- Aarsland D, Creese B, Politis M, Chaudhuri KR, Ffytche DH, Weintraub D, et al. Cognitive decline in Parkinson disease. *Nat Rev Neurol* 2017; 13: 217–31.
- Aggarwal CC, Hinneburg A, Keim DA. On the surprising behavior of distance metrics in high dimensional spaces. In *International Conference On Database Theory*. Berlin: Springer; 2001. p. 420–34.
- Allen EA, Damaraju E, Eichele T, Wu L, Calhoun VD. EEG signatures of dynamic functional network connectivity states. *Brain Topogr* 2018; 31: 101–16.
- Allen EA, Damaraju E, Plis SM, Erhardt EB, Eichele T, Calhoun VD. Tracking whole-brain connectivity dynamics in the resting state. *Cereb Cortex* 2014; 24: 663–76.
- Allen EA, Erhardt EB, Damaraju E, Gruner W, Segall JM, Silva RF, et al. A baseline for the multivariate comparison of resting-state networks. *Front Syst Neurosci* 2011; 5: 2.
- Amboni M, Tessitore A, Esposito F, Santangelo G, Picillo M, Vitale C, et al. Resting-state functional connectivity associated with mild cognitive impairment in Parkinson's disease. *J Neurol* 2015; 262: 425–34.
- Antonini A, Abbruzzese G, Ferini-Strambi L, Tilley B, Huang J, Stebbins GT, et al. Validation of the Italian version of the movement disorder society—unified Parkinson's disease rating scale. *Neurol Sci* 2012; 34: 683–7.
- Babiloni C, Del Percio C, Lizio R, Noce G, Cordone S, Lopez S, et al. Abnormalities of cortical neural synchronization mechanisms in subjects with mild cognitive impairment due to Alzheimer's and Parkinson's diseases: an EEG study. *J Alzheimers Dis* 2017; 59: 339–58.
- Baggio HC, Sala-Llonch R, Segura B, Marti MJ, Valldeoriola F, Compta Y, et al. Functional brain networks and cognitive deficits in Parkinson's disease. *Hum Brain Mapp* 2014; 35: 4620–34.
- Baggio HC, Segura B, Sala-Llonch R, Marti MJ, Valldeoriola F, Compta Y, et al. Cognitive impairment and resting-state network connectivity in Parkinson's disease. *Hum Brain Mapp* 2015; 36: 199–212.
- Bell AJ, Sejnowski TJ. An information-maximization approach to blind separation and blind deconvolution. *Neural Comput* 1995; 7: 1129–59.
- Berman BD, Smucny J, Wylie KP, Shelton E, Kronberg E, Leehey M, et al. Levodopa modulates small-world architecture of functional brain networks in Parkinson's disease. *Mov Disord* 2016; 31: 1676–84.
- Biundo R, Weis L, Facchini S, Formento-Dojot P, Vallelunga A, Pilleri M, et al. Cognitive profiling of Parkinson disease patients with mild cognitive impairment and dementia. *Parkinsonism Relat Disord* 2014; 20: 394–9.
- Calhoun VD, Adali T, Pearlson GD, Pekar J. A method for making group inferences from functional MRI data using independent component analysis. *Hum Brain Mapp* 2001a; 14: 140–51.
- Calhoun VD, Adali T, Pearlson GD, Pekar JJ. Spatial and temporal independent component analysis of functional MRI data containing a pair of task-related waveforms. *Hum Brain Mapp* 2001b; 13: 43–53.
- Cohen JR, D'Esposito M. The segregation and integration of distinct brain networks and their relationship to cognition. *J Neurosci* 2016; 36: 12083–94.
- Cordes D, Haughton VM, Arfanakis K, Wendt GJ, Turski PA, Moritz CH, et al. Mapping functionally related regions of brain with functional connectivity MR imaging. *AJNR Am J Neuroradiol* 2000; 21: 1636–44.
- Cordes D, Zhuang X, Kaleem M, Sreenivasan K, Yang Z, Mishra V, et al. Advances in functional magnetic resonance imaging data analysis methods using empirical mode decomposition to investigate temporal changes in early Parkinson's disease. *Alzheimers Dement* 2018; 4: 372–86.
- Damaraju E, Allen EA, Belger A, Ford JM, McEwen S, Mathalon DH, et al. Dynamic functional connectivity analysis reveals transient states of dysconnectivity in schizophrenia. *Neuroimage Clin* 2014; 5: 298–308.
- Daniel SE, Lees AJ. Parkinson's Disease Society Brain Bank, London: overview and research. *J Neural Transm* 1993; 39: 165–72.
- Demirtas M, Tornador C, Falcon C, Lopez-Sola M, Hernandez-Ribas R, Pujol J, et al. Dynamic functional connectivity reveals altered variability in functional connectivity among patients with major depressive disorder. *Hum Brain Mapp* 2016; 37: 2918–30.
- Diez-Cirarda M, Strafella AP, Kim J, Pena J, Ojeda N, Cabrera-Zubizarreta A, et al. Dynamic functional connectivity in Parkinson's disease patients with mild cognitive impairment and normal cognition. *Neuroimage Clin* 2018; 17: 847–55.
- Dubois B, Burn D, Goetz C, Aarsland D, Brown RG, Broe GA, et al. Diagnostic procedures for Parkinson's disease dementia: recommendations from the movement disorder society task force. *Mov Disord* 2007; 22: 2314–24.
- Elton A, Gao W. Task-related modulation of functional connectivity variability and its behavioral correlations. *Hum Brain Mapp* 2015; 36: 3260–72.
- Erhardt EB, Rachakonda S, Bedrick EJ, Allen EA, Adali T, Calhoun VD. Comparison of multi-subject ICA methods for analysis of fMRI data. *Hum Brain Mapp* 2011; 32: 2075–95.
- Esposito F, Tessitore A, Giordano A, De Micco R, Paccone A, Conforti R, et al. Rhythm-specific modulation of the sensorimotor network in drug-naïve patients with Parkinson's disease by levodopa. *Brain* 2013; 136: 710–25.
- Fox MD, Zhang D, Snyder AZ, Raichle ME. The global signal and observed anticorrelated resting state brain networks. *J Neurophysiol* 2009; 101: 3270–83.
- Friedman J, Hastie T, Tibshirani R. Sparse inverse covariance estimation with the graphical lasso. *Biostatistics* 2008; 9: 432–41.
- Gorges M, Muller HP, Lule D, Consortium L, Pinkhardt EH, Ludolph AC, et al. To rise and to fall: functional connectivity in cognitively normal and cognitively impaired patients with Parkinson's disease. *Neurobiol Aging* 2015; 36: 1727–35.
- Göttlich M, Munte TF, Heldmann M, Kasten M, Hagenah J, Kramer UM. Altered resting state brain networks in Parkinson's disease. *PLoS One* 2013; 8: e77336.
- Himberg J, Hyvarinen A, Esposito F. Validating the independent components of neuroimaging time series via clustering and visualization. *NeuroImage* 2004; 22: 1214–22.
- Hindriks R, Adhikari MH, Murayama Y, Ganzetti M, Mantini D, Logothetis NK, et al. Can sliding-window correlations reveal dynamic functional connectivity in resting-state fMRI? *Neuroimage* 2016; 127: 242–56.
- Hutchinson RM, Womelsdorf T, Allen EA, Bandettini PA, Calhoun VD, Corbetta M, et al. Dynamic functional connectivity: promise, issues, and interpretations. *NeuroImage* 2013; 80: 360v78.
- Jones DT, Vemuri P, Murphy MC, Gunter JL, Senjem ML, Machulda MM, et al. Non-stationarity in the “Resting Brain's” modular architecture. *PLoS One* 2012; 7: e39731.
- Katz S. Assessing self-maintenance: activities of daily living, mobility, and instrumental activities of daily living. *J Am Geriatr Soc* 1983; 31: 721–7.

- Kehagia AA, Barker RA, Robbins TW. Neuropsychological and clinical heterogeneity of cognitive impairment and dementia in patients with Parkinson's disease. *Lancet Neurol* 2010; 9: 1200–13.
- Kim J, Criaud M, Cho SS, Diez-Cirarda M, Mihaescu A, Coakeley S, et al. Abnormal intrinsic brain functional network dynamics in Parkinson's disease. *Brain* 2017; 140: 2955–67.
- Kulisevsky J, Fernandez de Bobadilla R, Pagonabarraga J, Martinez-Horta S, Campolongo A, Garcia-Sanchez C, et al. Measuring functional impact of cognitive impairment: validation of the Parkinson's disease cognitive functional rating scale. *Parkinsonism Relat Disord* 2013; 19: 812–7.
- Litvan I, Goldman JG, Tröster AI, Schmand BA, Weintraub D, Petersen RC, et al. Diagnostic criteria for mild cognitive impairment in Parkinson's disease: Movement Disorder Society Task Force guidelines. *Mov Disord* 2012; 27: 349–56.
- Liu F, Wang Y, Li M, Wang W, Li R, Zhang Z, et al. Dynamic functional network connectivity in idiopathic generalized epilepsy with generalized tonic-clonic seizure. *Hum Brain Mapp* 2017; 38: 957–73.
- Lloyd S. Least squares quantization in PCM. *IEEE Trans Inf Theory* 1982; 28: 129–37.
- Lottman KK, Kraguljac NV, White DM, Morgan CJ, Calhoun VD, Butt A, et al. Risperidone effects on brain dynamic connectivity-A prospective resting-state fMRI study in schizophrenia. *Front Psychiatry* 2017; 8: 14.
- Niethammer M, Eidelberg D. Metabolic brain networks in translational neurology: concepts and applications. *Ann Neurol* 2012; 72: 635–47.
- Nomi JS, Vij SG, Dajani DR, Steimke R, Damaraju E, Rachakonda S, et al. Chronnectomic patterns and neural flexibility underlie executive function. *Neuroimage* 2017; 147: 861–71.
- Olde Dubbelink KT, Stoffers D, Deijen JB, Twisk JW, Stam CJ, Hillebrand A, et al. Resting-state functional connectivity as a marker of disease progression in Parkinson's disease: a longitudinal MEG study. *Neuroimage Clin* 2013; 2: 612–9.
- Pedersen KF, Larsen JP, Tysnes OB, Alves G. Prognosis of mild cognitive impairment in early Parkinson disease: the Norwegian ParkWest study. *JAMA Neurol* 2013; 70: 580–6.
- Power JD, Barnes KA, Snyder AZ, Schlaggar BL, Petersen SE. Spurious but systematic correlations in functional connectivity MRI networks arise from subject motion. *Neuroimage* 2012; 59: 2142–54.
- Prodoehl J, Burciu RG, Vaillancourt DE. Resting state functional magnetic resonance imaging in Parkinson's disease. *Curr Neurol Neurosci Rep* 2014; 14: 448.
- Raichle ME. The brain's default mode network. *Annu Rev Neurosci* 2015; 38: 433–47.
- Rousseeuw PJ. Silhouettes: a graphical aid to the interpretation and validation of cluster analysis. *J Comput Appl Math* 1987; 20: 53–65.
- Roweis ST. EM algorithms for PCA and SPCA. *Advances in neural information processing systems*. Cambridge: MIT Press; 1998. p. 626–32.
- Schindlbeck KA, Eidelberg D. Network imaging biomarkers: insights and clinical applications in Parkinson's disease. *Lancet Neurol* 2018; 17: 629–40.
- Shirer WR, Ryali S, Rykhlevskaia E, Menon V, Greicius MD. Decoding subject-driven cognitive states with whole-brain connectivity patterns. *Cereb Cortex* 2012; 22: 158–65.
- Smith SM, Miller KL, Salimi-Khorshidi G, Webster M, Beckmann CF, Nichols TE, et al. Network modelling methods for FMRI. *NeuroImage* 2011; 54: 875–91.
- Tomlinson CL, Stowe R, Patel S, Rick C, Gray R, Clarke CE. Systematic review of levodopa dose equivalency reporting in Parkinson's disease. *Mov Disord* 2010; 25: 2649–53.
- Tomasi, DG, Shokri-Kojori, E, Volkow, ND. Temporal evolution of brain functional connectivity metrics: could 7 min of rest be enough? *Cerebral Cortex* 2016; 27: 4153–65.
- Van Dijk KR, Sabuncu MR, Buckner RL. The influence of head motion on intrinsic functional connectivity MRI. *Neuroimage* 2012; 59: 431–8.
- Varoquaux G, Gramfort A, Poline J-B, Thirion B. Brain covariance selection: better individual functional connectivity models using population prior. *Advances in neural information processing systems*; 2010; 2334–42.